Optimal cooling of a driven artificial atom in dissipative environment

Lingjie Du and Yang Yu*
National Laboratory of Solid State Microstructures and Department of Physics, Nanjing University, Nanjing 210093, China
(Dated: December 15, 2010)

We study microwave-driven cooling in a superconducting flux qubit subjected to environment noises. For the weak decoherence, our analytical results agree well with the experimental observations near the degeneracy point and show that the microwave amplitude for optimal cooling should depend linearly on the dc flux detuning. With the decoherence increasing, more vibrational degrees of freedom couple in, making the ordinary cooling method less effective or even fail. We propose an improved cooling method, which can eliminate the perturbation of additional vibrational degrees of freedom hence keep high efficiency even under the strong decoherence. Furthermore, we point out that the decoherence will modulate the frequency where microwave-driven Landau-Zener transition reaches maximum in both methods, displaying the feature of incoherent dynamics which is important for the optimal cooling of qubits and other quantum systems.

PACS numbers: 37.10.De,03.65.Yz,85.25.-j,03.67.Lx

I. INTRODUCTION

Superconducting devises based on Josephson tunnel junctions, shown to act as artificial atoms, can be used to demonstrate quantum phenomena at macroscopic scales and hold promise for applications in quantum computation as qubits.[1–5] Qubits are very delicate and their manipulation with electronics needs to be isolated from the disturbance of the environmental thermal noise.[6–20] Therefore, cooling the qubits, considered as a straightforward means to preserve the coherence of qubits, paves the way for remarkable achievements in demonstrating various quantum coherent phenomena. In general, the dilution refrigeration is used for cooling with some drawbacks such as limited cooling efficiency and poor heat conduction. Therefore, novel cooling techniques are required to improve the performance of qubits.

Recently an interesting technique, microwave-driven cooling, was developed from the extensive investigations on coupled systems of the qubits and quantum resonators. It was found that the qubit can cool down the resonator[21–24]. On the other hand, in a recent experiment, the inverse process, using a "resonator" to cool a qubit, was also proposed to lower the temperature of a superconducting flux qubit[25,26] by Valenzuela $et\ al$.[27]. At optimal cooling, they achieved the effective temperatures 3 mK, which was two orders of magnitude lower than the surrounding environment temperature, with the condition of the $amplitude$ where the particular flux amplitude made only one of two side crossovers reached and the $frequency$ of 5 MHz. This process is analogous to the optical sideband cooling,[28–31] where a two-level system (TLS) in an ion (an "internal" qubit) is used to cool ion trap potential (an "external" oscillator), subsequently providing direct cooling to the degrees of freedom of interest. But different from the optical method, here an ancillary "internal" oscillator-like state is coupled to an "internal" qubit by a side crossover, cooling the "internal" qubit through Microwave-driven Landau-Zener (MDLZ) transitions (or Landau-Zener-Stückelberg interferometry).[17,32,33] As the qubit is driven through a degeneracy point (or crossover), Landau-Zener (LZ) transition happens,[34] which usually is used to enhance the quantum tunneling rate,[35,36] to prepare the quantum states,[37] and to control the gate operations.[38] When a periodic strong driving is applied to the qubit, the qubit undergoes repeated LZ transitions at the degeneracy point. If the driving frequency is larger than the decoherence rate, the repetition of LZ transitions can induce quantum-mechanical interference, which leads to an oscillatory dependence of qubit population in the final state on the detuning from the degeneracy point and the microwave amplitude, known as Landau-Zener-Stückelberg (LSZ) interferometry.[17–19,27,39–48] When the decoherence rate is larger than the driving frequency, the interference patterns are nearly washed out. Due to the loss of coherence, this incoherent region draws little attention in quantum information until the microwave-driven cooling emerges.[27]

In this paper, firstly we obtain the optimal cooling conditions in Ref. [27] based on a microscopic model of LZS interferometry in the multi-level system.[47] Besides only one crossover reaches, the microwave $amplitude$ for optimal cooling should be linearly dependent on the dc flux detuning. Moreover, the $frequency$ condition also varies slightly with different detunings. Then we investigate how the decoherence modifies the condition for optimal cooling. The strong decoherence might couple the "internal" qubit to another "internal" oscillator-like state which would interact with the original oscillator-like state, destroying the cooling effect although controlled amplitude makes only one of two side crossovers reached. To realize the cooling under the strong decoherence, we propose an exquisite microwave manipulation to exclude the excessive oscillator-like state which demolishes the cooling in MDLZ transitions. Active cooling of qubits provides an effective means for qubit state preparation even under the strong decoherence and for suppressing the decoherence in multi-qubit systems. Especially, it can be applied to refrigerate environmental degrees of freedom[49] and cool neighboring quantum systems.[50] Additionally, for systems consist of the interaction between the qubit and the real resonator, such as micromechanical beam, this method can also be used to cool down the qubit, or even resonators. We also find that the frequency for optimal cooling relies on the decoherence, not always achieved at the extremely low frequency. The decoherence will modulate the frequency corresponding to the maximum rate of MDLZ transition, leading the change of the

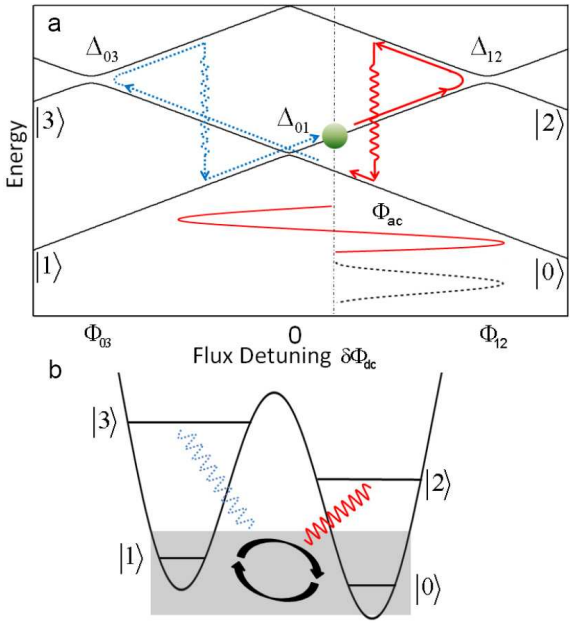

FIG. 1: (Color online). Schematic energy diagram of a multi-level superconducting flux qubit. (a). Red solid curve represents the microwave Φ_{ac} in the ordinary cooling method in Sec. III. Black dashed curve represents the microwave in the new cooling method in Sec. IV. The dashed black line expresses a particular static flux detuning $\delta\Phi_{dc}$. The symmetry makes $|\Phi_{12}| = |\Phi_{03}|$. States $|1\rangle$ and $|3\rangle$ are in the left well; $|0\rangle$ and $|2\rangle$ are in the right well. The red solid path describes the cooling with the population in state $|1\rangle$ transferred to $|0\rangle$. The blue dot path represents the population transferred from state $|0\rangle$ to $|1\rangle$. (b). The shaded region describes the "internal" qubit. Conventionally, we employ a microwave to couple a oscillator-like state $|2\rangle$ to the "internal" qubit. However, the strong decoherence would make another oscillator-like state $|3\rangle$ destroys the cooling completely, although state $|3\rangle$ has little effect under the weak decoherence.

$frequency$ condition in both methods. At the strong decoherence environment, LZS interference displays the stationary population of incoherent evolution. While the trend of the quantum information is coherent manipulation, our analysis shows the importance of the incoherent LZS dynamics in quantum cooling.

The organization of this paper is as follows. In Sec. II, we give the basic model of LZS interferometry, including LZ transition and the rate equation. Then we divide the cooling region into two regions and the incoherent transition region is introduced. In Sec. III, we present a detailed analysis of the optimal cooling in the experiment and find that there are different $amplitude$ conditions for optimal cooling at different detunings, besides the change of the $frequency$ condition. In Sec. IV, we study the cooling under the strong decoherence, and find that the strong decoherence makes the cooling ineffective in the ordinary method. Then we propose an improved cooling method to solve the problem and discuss the optimal cooling in the new method. In Sev. V, we study the relation between the efficiency of MDLZ transition and the decoherence, explaining abnormal phenomena.

II. BASIC MODEL

We focus on a multi-level superconducting flux qubit, which consists of a superconducting loop interrupted by three Josephson junctions[17,27,41] (Fig. 1). If the external flux bias $\Phi \approx 0.5\Phi_0$, where $\Phi_0 = h/2e$ is the flux quantum, a double well landscape of the potential energy parameterized by the dc flux detuning $\delta\Phi_{dc} = \Phi - 0.5\Phi_0$ exists in the flux qubit. In the millikelvin temperature ~ 10 mK, a series of diabatic states, denoted as $|i\rangle$ and $|j\rangle$, respectively are localized in different wells with the crossovers Δ_{ij} between states $|i\rangle$ and $|j\rangle$ (i = 0, 2, right well with negative slope; j = 1, 3, left well with positive slope). We assume the barrier is relatively high thus the tunneling strength (Δ_{ij}) is small. The two wells correspond to different flowing directions of the persistent currents, namely clockwise and anticlockwise. $\delta\Phi_{ij}$ is the flux detuning, at which the crossover Δ_{ij} is reached. As the qubit is driven with a microwave $\Phi_{ac} = \Phi_{rf}\sin\omega t$, where Φ_{rf} is the microwave amplitude, the time dependent flux detuning is

$$\delta\Phi(t) = \delta\Phi_{dc} + \Phi_{ac} = \delta\Phi_{dc} + \Phi_{rf}\sin\omega t.$$

Then the time dependent energy of eigenstate $|i\rangle$ can be described as

$$\begin{aligned}\varepsilon_i(t) &= \varepsilon_i^* \pm m_i\delta\Phi(t)\\ &= \varepsilon_i^* \pm m_i(\delta\Phi_{dc} + \Phi_{rf}\sin\omega t),\end{aligned}$$

where ε_i^* is the energy spacing between state $|i\rangle$ and the lowest state in the same well at $\delta\Phi(t) = 0$ mΦ_0, $\varepsilon_i = \varepsilon_i^* \pm m_i\delta\Phi_{dc}$ is the dc energy of eigenstate $|i\rangle$, (+ corresponds the states in the left well, $-$ corresponds the states in the right well), and $m_i = dE_i(\Phi)/d\Phi$ is the energy level slope of $|i\rangle$.

When the state $|i\rangle$ is driven through the crossover Δ_{ij} at the time $t = t_0$, the probability of LZ transition from state $|i\rangle$ to $|j\rangle$ is given by (we set $\hbar = k_B = 1$)

$$p = 1 - \exp(-\frac{\Delta_{ij}^2}{4\zeta}), \tag{1}$$

where the relative-energy sweep rate $\zeta = \frac{d}{dt}[|\varepsilon_i(t) - \varepsilon_j(t)|]|_{t=t_0}$. For the case of the periodic sinusoidal driving, we have $|\varepsilon_i(t) - \varepsilon_j(t)| = (|m_i| + |m_j|)\Phi_{rf}\sin\omega t$ and $\zeta = (|m_i| + |m_j|)\omega\Phi_{rf}|\cos\omega t_0|$. Therefore $\zeta \propto \omega$, which means larger frequency leads to less probability of LZ transition.

To describe a driven multi-level qubit system interacting with a dissipative environment, we consider the Hamiltonian

$$H = H_0 + H_{int} + H_B, \tag{2}$$

where $H_0 = \sum_{i\neq j}\frac{\Delta_{ij}}{2}|i\rangle\langle j| + \sum_k \varepsilon_k(t)|k\rangle\langle k|$ is the Hamiltonian of the multi-level qubit, H_{int} is the system-environment interaction Hamiltonian, and H_B is the environment Hamiltonian. Considering the noise from the environment, we assume the linear coupling between the qubit operators and environ-

ment operator[51,52]

$$H_{int} = -\frac{Q}{2} \sum_{\substack{|i\rangle\in\text{right well}\\ |j\rangle\in\text{left well}}} (|i\rangle\langle i| - |j\rangle\langle j|) + \sum_{k\neq k'} \phi_{kk'}(|k\rangle\langle k'| + |k'\rangle\langle k|)Q, \quad (3)$$

where Q is the operator of environment noise, states $|k\rangle$ and $|k'\rangle$ belong to the same well and $\phi_{kk'}$ is the coupling matrix element. The first term describes the dephasing from low frequency noise. The second term $H_{hf} = \sum_{k\neq k'} \phi_{kk'}(|k\rangle\langle k'| + |k'\rangle\langle k|)Q$ represents the effect of high frequency noise to produce the intrawell relaxation.

To describe the long-time system evolution, we can employ the rate equation approach. In this case, MDLZ transition between two states in opposite wells needs to be considered. Starting from the Hamiltonian (2), we use the Gaussian white noise model and perturbation theory[45,47,53] to derive MDLZ transition rate from state $|i\rangle$ to $|j\rangle$ as

$$W_{ij} = \frac{\Delta_{ij}^2}{2} \sum_n \frac{(\Gamma_2+\gamma)J_n^2(A_{ij}/\omega)}{(\varepsilon_{ij}-n\omega)^2+(\Gamma_2+\gamma)^2}, \quad (4)$$

where $\varepsilon_{ij} = \varepsilon_i - \varepsilon_j$ is the dc energy detuning of states $|j\rangle$ and $|i\rangle$, $A_{ij} = |m_i|\Phi_{rf} + |m_j|\Phi_{rf}$ is the energy amplitude of the microwave, Γ_2 is the dephasing rate, $\gamma = (\Gamma_{j1} + \Gamma_{i0})/2$, Γ_{j1} and Γ_{i0} are the intrawell relaxation rate from states $|j\rangle$ and $|i\rangle$ in the left and right well respectively. Of course, when i=0 or j=1, the corresponding Γ_{i0} or Γ_{j1} is zero. The term $\Gamma_2+\gamma$ describes the decoherence in this sub-system composed of states $|j\rangle$ and $|i\rangle$. In this article, when considering different decoherence, we would hold the intrawell relaxation rate $\Gamma_{31} = \Gamma_{20} = 2\pi \times 0.1$ GHz,[47] only changing and mentioning the dephasing rate.

In order to analyze the optimal cooling, we consider four lowest states in which the qubit state occupations $p_i (i = 0, 1, 2, 3)$ follow

$$\begin{aligned}
\dot{p}_{00} &= -p_{00}(\Gamma_{01}^{'} + W_{03} + W_{01}) + (\Gamma_{10}^{'} + W_{10})p_{11} + W_{30}p_{33} + \Gamma_{20}p_{22} \\
\dot{p}_{11} &= -p_{11}(\Gamma_{10}^{'} + W_{12} + W_{10}) + (\Gamma_{01}^{'} + W_{01})p_{00} + \Gamma_{31}p_{33} + W_{21}p_{22} \\
\dot{p}_{22} &= -p_{22}(\Gamma_{20} + W_{21} + W_{23}) + W_{32}p_{33} + W_{12}p_{11} \\
p_{00} &+ p_{11} + p_{22} + p_{33} = 1, \quad (5)
\end{aligned}$$

where $\Gamma_{10}^{'}$, $\Gamma_{01}^{'} = \Gamma_{10}^{'}\exp(-\varepsilon_{01}/T)$ is the down and up interwell relaxation rate between states $|1\rangle$ and $|0\rangle$, and T is the temperature of the environment.

In the microwave-driven sideband cooling, states $|0\rangle$ and $|1\rangle$ are the two lowest states, which are far below the other states and form an "internal" qubit. The state $|2\rangle$ is treated as an ancillary "internal" oscillator-like state, which is localized in the same well with state $|0\rangle$, and Δ_{12} is considered as the side crossover. If the qubit is in equilibrium with the environment, the population in state $|1\rangle$ is excited from state $|0\rangle$

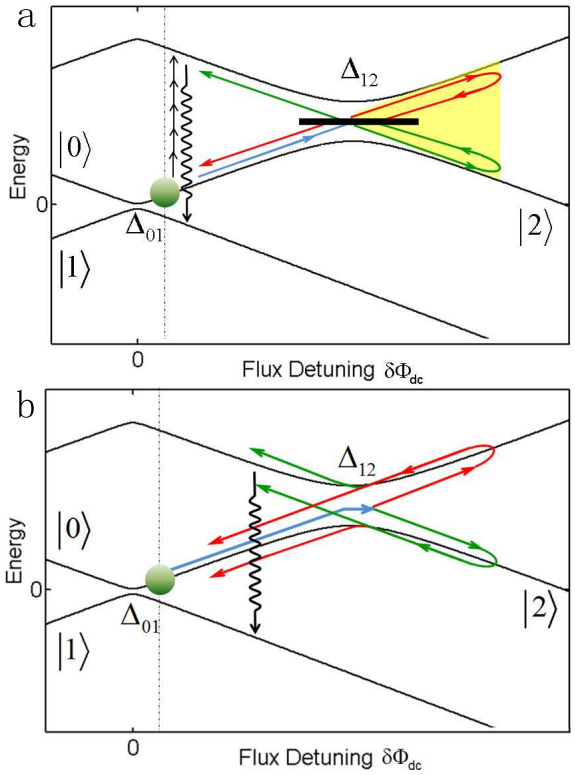

FIG. 2: (Color online). Schematic energy diagram illustrating the cooling regions. In (a), the solid line expresses the transition from state $|1\rangle$ to $|0\rangle$ at the coherent region. The arrows mark well-resolved resonances of n-photon transition observed under the high frequency driving. The shaded region expresses the interference phase. In (b), the coherence interference vanishes and the transition from state $|1\rangle$ to $|0\rangle$ is realized at the incoherent transition region.

thermally following the Boltzmann relation

$$p_{11}/p_{00} = \exp(-\varepsilon_{10}/T). \quad (6)$$

This expression shows the influence of temperature is large at small detunings near 0 mΦ_0, which thereby becomes main cooling interests. As shown in Fig. 1(a), by repeated LZ transitions, the microwave drives the unwanted thermal population in state $|1\rangle$ to $|2\rangle$, whose population relaxes fast into state $|0\rangle$. Then the population transferred to state $|0\rangle$ faster than the thermal repopulation of state $|1\rangle$, cools the "internal" qubit. As indicated from Eq. (6), less population in state $|1\rangle$ corresponds to lower effective temperature. Hence we can use the population in state $|1\rangle$ to determine the effective temperature realized by microwave cooling.

Microwave-driven sideband cooling depends on MDLZ transition from state $|1\rangle$ to $|2\rangle$ which exhibits a rich structure as a function of the microwave frequency. Therefore we divide the cooling into two regions by the frequency. As shown in Fig. 2 (a), at the coherent region where the frequency is larger than the decoherence rate $\Gamma_2+\gamma$, the qubit state is split into the coherent superposition of states $|1\rangle$ and $|2\rangle$ by the crossover Δ_{12}. Then a phase difference is constructed to form the quantum interference.[17] Especially at high frequencies near several

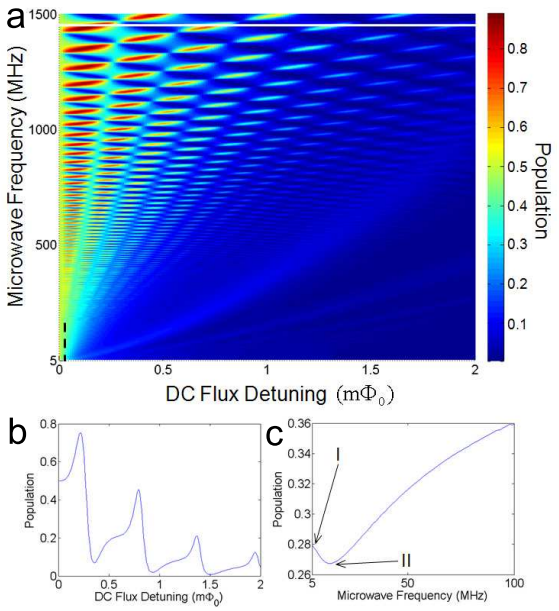

FIG. 3: (Color online). The population in state $|1\rangle$ versus flux detuning and microwave frequency with the flux amplitude $\Phi_{rf} = 8.4$ mΦ_0. The locations of the crossovers Δ_{01},and Δ_{12} are 0 mΦ_0, and 8.4 mΦ_0, respectively. The diabatic energy-level slope $|m_0|(|m_1|)$ =$2\pi \times 1.44$ GHz/mΦ_0, and $|m_2|(|m_3|)$ =$2\pi \times 1.09$ GHz/mΦ_0. $\Delta_{01}/2\pi = 0.013$ GHz, $\Delta_{03}/2\pi = \Delta_{12}/2\pi = 0.09$ GHz. The parameters above are from the experiment.[41] Furthermore we estimate $\Delta_{23}/2\pi = 0.5$ GHz. The dephasing rate we used in calculation $\Gamma_2/2\pi = 0.06$ GHz, the intrawell relaxation rate $\Gamma_{20}/2\pi = \Gamma_{31}/2\pi = 0.1$ GHz,[47] and the interwell relaxation $\Gamma'_{10}/2\pi = 0.00005$ GHz. The environment temperature T is 50 mK. (b). The population in state $|1\rangle$ versus the microwave frequency at the detuning 0.05 mΦ_0. (c) The population in state $|1\rangle$ versus flux detuning at the frequency 1460 MHz.

subgigahertzes, the well resolved n-photon resonances are observed. At the incoherent region with the frequency is lower than the decoherence rate, as state $|1\rangle$ is driven through the crossover Δ_{12}, the state is split into the coherent superposition of states $|1\rangle$ and $|2\rangle$ by LZ transition. However the decoherence eliminates its coherence quickly such that the superposition becomes the incoherent mixture, as illustrated in Fig. 2 (b). When the microwave drives the state back to Δ_{12}, the second LZ transition occurs, but state $|1\rangle$ split from state $|1\rangle$ would not interfere with state $|1\rangle$ split from state $|2\rangle$ due to the lost coherence. In next sections we will show this region has a important role in the optimal microwave cooling.

III. OPTIMAL COOLING UNDER THE WEAK DECOHERENCE

In the experiment under the weak decoherence,[27] e. g. $\Gamma_2/2\pi = 0.06$ GHz and $\gamma/2\pi = 0.05$ GHz, Valenzuela $et\ al$ proposed that the optimal cooling near the degeneracy point was realized at the flux amplitude $\Phi_{rf} = \Phi_{12} = 8.4$ mΦ_0 and the frequency ~ 5 MHz.

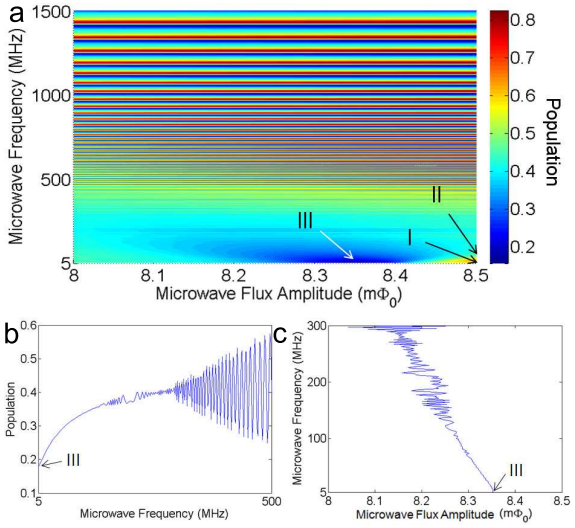

FIG. 4: (Color online). (a) The population in state $|1\rangle$ versus microwave frequency and flux amplitude with the detuning $\delta\Phi_{dc} = 0.05$ mΦ_0. The other parameters used are the same with those of Fig. 3. (b) The lowest population extracted from (a) at each frequency versus microwave frequency. (c) The amplitude corresponding to the lowest population extracted from (a) at each frequency versus microwave frequency.

In the stationary case, $\dot{p}_{22} = \dot{p}_{11} = \dot{p}_{33} = \dot{p}_{00} = 0$, with the amplitude $\Phi_{rf} = 8.4$ mΦ_0 we use the rate equation Eq. (5) to plot the population in state $|1\rangle$ at different detunings and frequencies as shown in Fig. 3 (a). At the coherent region the effective cooling can only be achieved at some detunings, [Fig. 3 (b)] such that we do not consider the coherent region in microwave cooling. At the incoherent transition region, lower frequency leads to less population in state $|1\rangle$ at all detunings, which means more efficient cooling. These results agree with the experimental observations.[27] Then we extract the data in the detuning $\delta\Phi_{dc} = 0.05$ mΦ_0 [the black dashed line in Fig. 3(a)] for detailed analysis in Fig. 3 (c). When the frequency is less than 100 MHz, the behavior of population dependent on the frequency follows the above discussion. However, as the frequency reaches 10 MHz, the optimal cooling at this detuning is realized (point II). Then at point I where the frequency is 5 MHz, the population is larger than that at point II. This result suggests that the condition for optimal cooling obtained by the experiment is not sufficiently optimized.

To explain the behavior exhibited in Fig. 3, we make a comprehensive analysis by varying microwave amplitudes and frequencies at the detuning $\delta\Phi_{dc} = 0.05$ mΦ_0, and show the population in state $|1\rangle$ in Fig. 4 (a). In detail, we extract the lowest population and the corresponding amplitudes at different frequencies, as shown in Fig. 4 (b) and Fig. 4 (c) respectively. Seen from Fig. 4 (b), the population in state $|1\rangle$ displays a monotonic decrease with the frequency and the lowest population at the detuning $\delta\Phi_{dc} = 0.05$ mΦ_0 is realized at point III with 5 MHz and the corresponding amplitude 8.35 mΦ_0, instead of I, or II [Fig. 4 (c)]. As a result, at the detuning $\delta\Phi_{dc} = 0.05$ mΦ_0 the frequency condition for optimal cooling is consistent with that of the experiment, while the

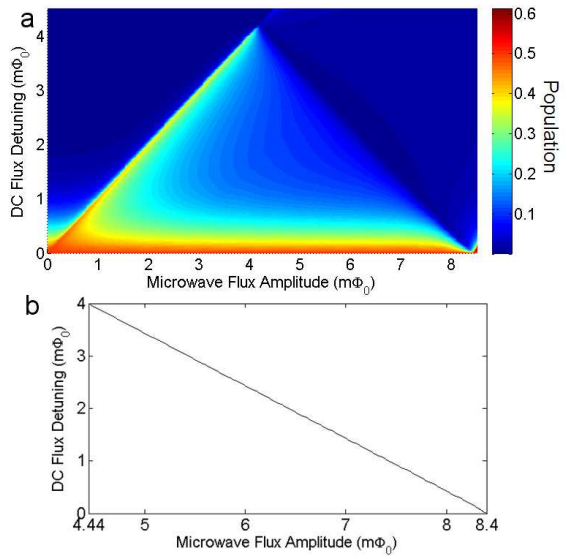

FIG. 5: (Color online). (a) The population in state $|1\rangle$ versus flux detuning and microwave flux amplitude with the frequency 5 MHz. The other parameters are identical with those of Fig. 3. (b) The amplitude corresponding to the lowest population extracted from (a) at each detuning versus the detuning.

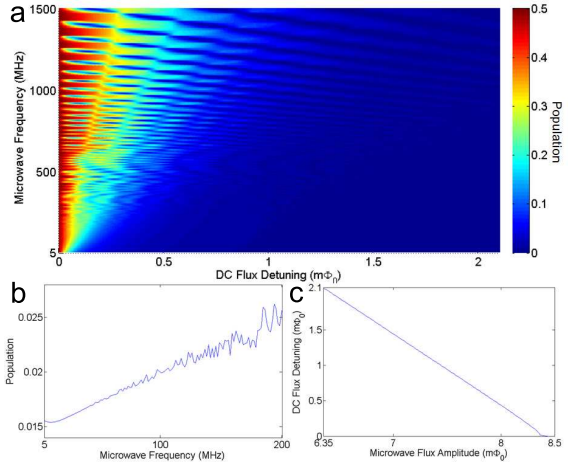

FIG. 6: (Color online). (a) The lowest population in state $|1\rangle$ among different flux amplitudes versus the frequency and detuning. The other parameters used are the same with those of Fig. 3. (b). The population in (a) versus the frequency at the detuning 0.5 mΦ_0. (c). The amplitude corresponding to the lowest population extracted from (a) at each detuning versus the detuning.

amplitude condition not.

Then at 5 MHz, we plot the population versus flux detuning and amplitude, shown in Fig. 5 (a). At each detuning, we extract the amplitude corresponding to the lowest population, as shown in Fig. 5 (b). The effective cooling is realized with the amplitude $\Phi_{rf} \gtrapprox \Phi_{12} - \delta\Phi_{dc}$, where $\Phi_{rf} + \delta\Phi_{dc} \approx 8.4$ mΦ_0 at the detuning near $\delta\Phi_{dc} = 0$ mΦ_0 and $\Phi_{rf} + \delta\Phi_{dc} \approx 8.45$ mΦ_0 at other detunings. (quantitive result of cooling can be seen in Fig. 8) Therefore, at the detuning approaching to 0 mΦ_0, the amplitude condition can be changed to $\Phi_{rf} = \Phi_{12}$, just as those demonstrated in Ref. [27].

Further, we extend the above discussion to all detunings. Firstly, following the similar way to obtain Fig. 4 (b), we change the amplitude to obtain the lowest population at each detuning and frequency, shown in Fig. 6 (a). At each detuning, the frequency 5 MHz always produces an efficient cooling. If we extract the data at the detuning $\delta\Phi_{\rm dc} = 0.5$ mΦ_0, a strange phenomenon that the population at 10 MHz is slightly less than that at 5 MHz can be observed [Fig. 6 (b)]. It should be mentioned that this case is different from the result in Fig. 3(c) which occurs at the amplitude 8.4 mΦ_0. The explanation would be given in Sec. V. Then we take account of the lowest population at other detunings. At these detuning, our calculation shows that the frequencies corresponding to the lowest population are always near 5 MHz and the difference between the population of 5 MHz and the lowest population is small. Therefore we can still accept the previous frequency condition for optimal cooling in practice. Moreover, the amplitude corresponding to the lowest population at each detuning is shown in Fig. 6 (c) and accords with that in Fig. 5 (b).

In the stationary case, considering $W_{12}, W_{03} \ll \Gamma_{31}, \Gamma_{20}$, the population in state $|1\rangle$ would be obtained as

$$p_{11} = \frac{\Gamma_{01}^{'} + W_{03}}{\Gamma_{10}^{'} + \Gamma_{01}^{'} + W_{12} + W_{03}}. \tag{7}$$

When the dc flux detuning is large, $W_{12}, \Gamma_{01}^{'} \gg W_{03}$ such that W_{03} can be neglected in Eq. (7) and the population in state $|1\rangle$ would depend on W_{12}. Firstly, we discuss the amplitude condition for optimal cooling. MDLZ transition rate W_{12} can be treated as the population transferred from state $|1\rangle$ to $|2\rangle$ in one unit time. Therefore W_{12} depends on the population transferred by one time of LZ transition in the crossover Δ_{12}, and the frequency which determines how many times of LZ transitions occur in one unit time. It is assumed that in the dc flux detuning far away from the crossover Δ_{12} there is nearly no tunneling transition between states $|1\rangle$ and $|2\rangle$, which is given by transition rate[51]

$$\Gamma = \frac{\Delta_{12}^2}{2} \frac{(\Gamma_2 + \gamma)}{\varepsilon_{12}^2 + (\Gamma_2 + \gamma)^2}, \tag{8}$$

where $\gamma = \Gamma_{20}/2$. Eq. (8) indicates the tunneling can be considered in a transition region $|\varepsilon_{12}| \lesssim \Gamma_2 + \gamma$, where $\Gamma \sim \Delta_{12}^2/[2(\Gamma_2 + \gamma)]$. Therefore longer time staying in the transition region in a period would contribute to larger population transferred from state $|1\rangle$ to $|2\rangle$ and better cooling efficiency. The long time staying in the transition region means a small velocity. At the same time, the velocity of a sinusoidal movement is the smallest when it closes to its full amplitude. Therefore, the amplitude which just reaches the transition region would bring the largest transition rate from state $|1\rangle$ to $|2\rangle$. When the decoherence is weak, the transition region is always near the crossover. As a result, we have the amplitude relation $\Phi_{rf} \gtrapprox \Phi_{12} - \delta\Phi_{dc}$ as obtained above. This relation also ensures that only the side crossover Δ_{12} reached.

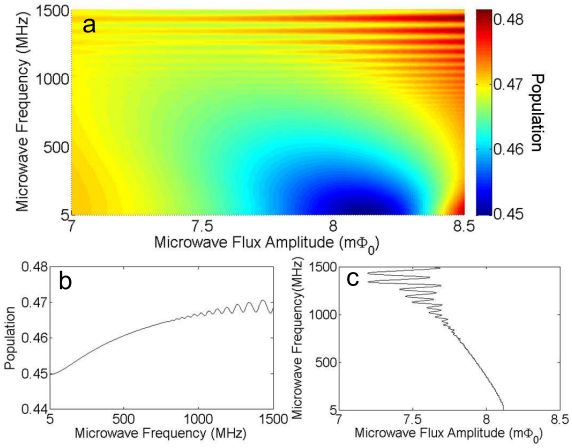

FIG. 7: (Color online). (a) The population in state $|1\rangle$ versus microwave frequency and flux amplitude with the detuning $\delta\Phi_{dc} = 0.05$ mΦ_0 and the dephasing rate $\Gamma_2/2\pi = 1$ GHz. The other parameters used are the same with those of Fig. 3. (b) The lowest population extracted from (a) at each frequency versus microwave frequency. (c) The amplitude corresponding to the lowest population extracted from (a) at each frequency versus microwave frequency.

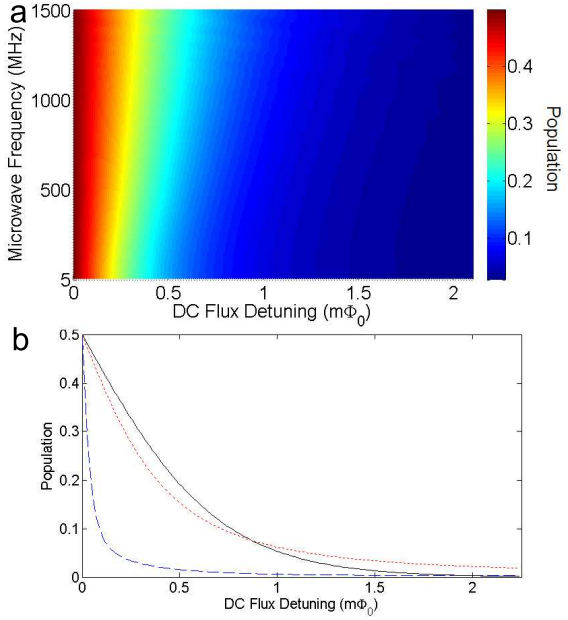

FIG. 8: (Color online) (a) The lowest population in state $|1\rangle$ among different flux amplitudes versus the frequency and detuning under the dephasing rate $\Gamma_2/2\pi = 1$ GHz. The other parameters used are the same with those of Fig. 3. (b). The comparison between the lowest population in state $|1\rangle$ at 5 MHz and each detuning under different dephasing rates (blue dashed line corresponds to $\Gamma_2/2\pi = 0.06$ GHz while red dotted line corresponds to $\Gamma_2/2\pi = 1$ GHz). The solid line represents the population in the equilibrium with the temperature 50 mK.

On the other hand, if we increase the frequency, smaller period indicates more times of LZ transitions in one unit time so as to cause a larger MDLZ transition rate. However, larger frequency results into larger velocity and shorter time in the transition region. Therefore it may also lead to smaller population transferred by LZ transition, shown in Eqs. (1) and (8). Consequently, the final result is complex and it is hard to determine the frequency condition for optimal cooling which would be discussed in Sec. V.

IV. NEW COOLING METHOD UNDER THE STRONG DECOHERENCE

Although the precise microwave manipulation can avoid reaching the another side crossover Δ_{03} thus eliminating the effect of state $|3\rangle$ in the cooling cycle, the strong decoherence may still couple states $|0\rangle$ and $|1\rangle$ to state $|3\rangle$[42,47]. State $|3\rangle$ would act as another "internal" oscillator-like state and destruct the cooling through MDLZ transition in Δ_{03}, shown in Fig. 1 (b). While the microwave drives the state near the side crossover Δ_{03}, LZ transition would transfer the population from state $|0\rangle$ to $|3\rangle$, which then relaxes into state $|1\rangle$. In this path, state $|3\rangle$ yields an inverse effect to destroy the cooling. The steady population in state $|1\rangle$ would be described by Eq. (7).

Under the strong decoherence, e. g. $\Gamma_2/2\pi = 1$ GHz and $\gamma = 0.05$ GHz, Fig. 7 (a) is the contour plot of the population in state $|1\rangle$ at the detuning $\delta\Phi_{dc} = 0.05$ mΦ_0 with different amplitudes and frequencies. For each frequency, we extract the lowest population and the corresponding amplitude, shown in Fig. 7 (b) and (c) respectively. Although even under the strong decoherence the cooling at this detuning still realizes the max efficiency at 5 MHz, the decoherence makes the population near 0.5 and the cooling very inefficient. At each detuning and frequency, we change the amplitude to obtain the lowest population in state $|1\rangle$ as shown in Fig. 8 (a). Then we extract the lowest population at 5 MHz from Fig. 8 (a) and plot them as the red dotted line in Fig. 8 (b). The population of optimal cooling under the strong decoherence is comparable with the population in the equilibrium, or even worse. The blue dashed line represents the lowest population at 5 MHz under the weak decoherence with $\Gamma_2/2\pi = 0.06$ GHz. Therefore, the comparison in Fig. 8 (b) shows that another oscillator-like state $|3\rangle$ counteracts the effect of original oscillator-like state $|2\rangle$.

At the same time, Fig. 7 (c) shows that the optimal cooling at the detuning 0.05 mΦ_0 is realized with the amplitude 8.1 mΦ_0 and frequency 5 MHz. In this case, the state does not reach the side crossover Δ_{12} and the result violates the amplitude condition we obtained in Sec. III. The strong decoherence would result in a large transition region near Δ_{12}. Subsequently in order to realize better cooling larger amplitude is needed. However larger amplitude would also drive the state closer to Δ_{03}. Moreover the strong decoherence enlarges the transition region near Δ_{03} such that the population transferred from state $|0\rangle$ to $|3\rangle$ is not able to be neglected, which then relaxes into state $|1\rangle$ and causes increasing population in state $|1\rangle$. Therefore, if the amplitude is decreased to minimize the efficiency of state $|3\rangle$, although the microwave does not completely cover the transition region near Δ_{12}, the

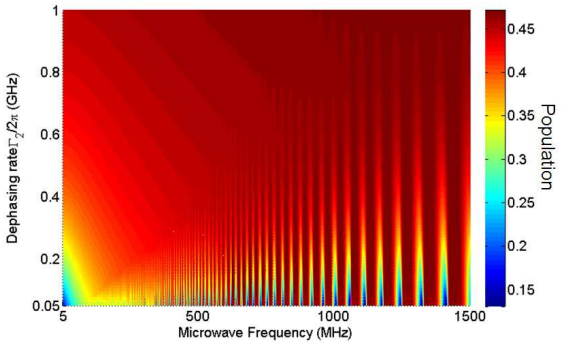

FIG. 9: (Color online). The lowest population in state $|1\rangle$ among different amplitudes versus dephasing rate and microwave frequency at the detuning $\delta\Phi_{dc}$ =0.05 mΦ_0. The other parameters used here are the same with those of Fig. 3.

final cooling efficiency may be better. By the way, under the weak decoherence, the amplitude condition at the detuning near the degeneracy point, e. g. $\delta\Phi_{dc} = 0.05$ mΦ_0, is different from that at detuning far away from the degeneracy point, e. g. $\Phi_{rf} + \delta\Phi_{dc} \approx 8.45$ mΦ_0 in Fig. 5 (b). That is because at the detuning near the degeneracy point the condition $\Phi_{rf} + \delta\Phi_{dc} \approx 8.45$ mΦ_0 would also make Δ_{03} involved hence destructing the optimal cooling. Therefore, the final amplitude condition is revised to $\Phi_{rf} + \delta\Phi_{dc} \approx 8.4$ mΦ_0 to minimize the effect of W_{03}.

At the detuning $\delta\Phi_{dc} = 0.05$ mΦ_0, we change amplitudes to extract the lowest population at different frequencies and dephasing rates, shown in Fig. 9. Independent of the decoherence, smaller frequency results into better cooling. Moreover, the dephasing rate larger than $2\pi \times 0.1$ GHz would easily destroy the cooling. It should be mentioned that in previous studies[41,47] the large amplitude microwave drives the system through the crossover Δ_{03}, coupling the two lowest states to state $|3\rangle$. However here instead of the large amplitude, the strong decoherence couples state $|3\rangle$ to the two lowest states. As shown in Figs. (7) and (8), in the case of the strong decoherence, decreasing the amplitude can not keep away from the influence of state $|3\rangle$. Therefore, new method is needed for the efficient cooling.

In the ordinary cooling cycle, at the beginning the sinusoidal microwave drives the state in the direction to the side crossover Δ_{12} and after going back to the initial detuning, the state is also driven in the direction to another side crossover Δ_{03}. Just the latter process brings the coupling to state $|3\rangle$. Therefore if we cancel the latter process, the cooling would come back. That means when the state goes back to the initial position, the microwave drives it still in the direction to Δ_{12}, not Δ_{03}. This seems a minor change but brings great efficiency to the cooling. It is worth to point out that the technique is readily available[43], making our method practical. We also can use periodic triangular waveform to drive the state. But to calculate conveniently, we still use the harmonic waveform shown in Fig. 1 (a). Then in Eq. (4), MDLZ transition

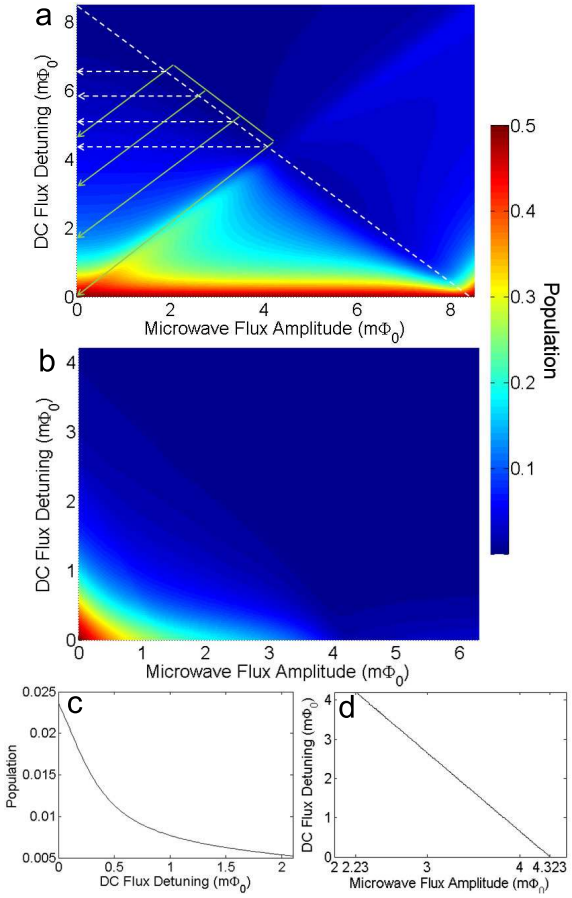

FIG. 10: (Color online). (a) The population in state $|1\rangle$ versus flux amplitude and detuning with the frequency 5MHz and the dephasing rate $\Gamma_2/2\pi = 1$ GHz in the original cooling method. The other parameters are identical with those of Fig. 3. The white dashed line indicates the optimal cooling region in the original method. The green solid line expresses the optimal cooling region in the new method. (b). The population in state $|1\rangle$ versus the flux amplitude and detuning in the same condition with (a) under the new method. (c) and (d). The lowest population and the corresponding amplitude extracted from (b) at each detuning versus the flux detuning.

rate can be changed to

$$W_{ji} = W_{ij} = \frac{\Delta_{ij}^2}{2} \sum_n \frac{(\Gamma_2+\gamma) J_n^2(A_{ij}/\omega)}{(\varepsilon_{ij}+A_{ij}-n\omega)^2+(\Gamma_2+\gamma)^2}, \qquad (9)$$

where state $|i\rangle$ and $|j\rangle$ are in the left and right well respectively, and ε_{ij} has the same definition as Eq. (4). Furthermore, $\Gamma_{01}^{'} = \Gamma_{10}^{'} \exp\{-(\varepsilon_{12} - A_{12})/T\}$. When the frequency is 5 MHz and the dephasing rate is $2\pi \times 1$ GHz, we use the ordinary cooling method to obtain the population distribution in state $|1\rangle$ at different amplitudes and detunings as shown in Fig. 10 (a). Fig. 10 (b) is the contour plot of the population in state $|1\rangle$ with the new method in the same condition as that in Fig. 10 (a). Extracting the lowest population in Fig. 10 (b) and its corresponding amplitude at each detuning as shown in Fig. 10 (c) and Fig. 10 (d) respectively, we find the cooling efficiency in the new method is much better than that in the or-

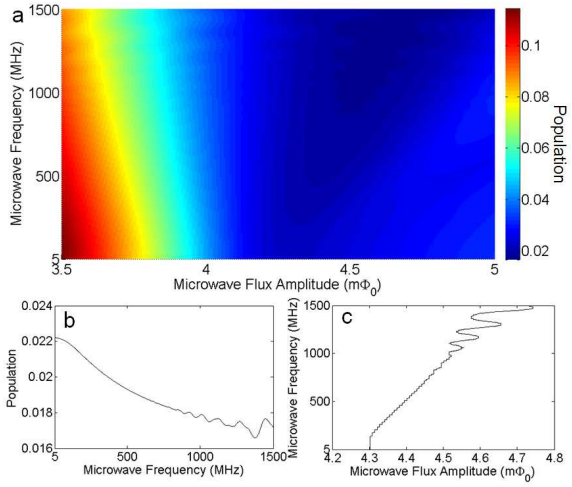

FIG. 11: (Color online). (a) The population in state $|1\rangle$ versus the frequency and flux amplitude with the detuning $\delta\Phi_{dc} = 0.05$ mΦ_0 and the dephasing rate $\Gamma_2/2\pi = 1$ GHz in the new method. The other parameters used are the same with those of Fig. 3. (b) and (c). The lowest population in state $|1\rangle$ extracted from (a) at each frequency and the corresponding amplitude versus microwave frequency.

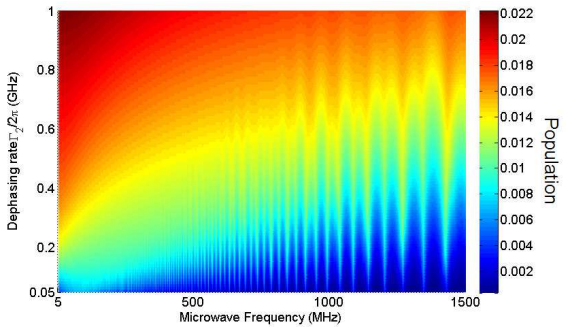

FIG. 12: (Color online). The lowest population in state $|1\rangle$ among different amplitudes versus the dephasing rate and microwave frequency at the detuning $\delta\Phi_{dc}$ =0.05 mΦ_0 in the new method. The parameters used here are the same with those of Fig. 3.

dinary method shown in Fig. 8 (b) especially at the detuning near 0 mΦ_0. Without the influence of Δ_{03}, the amplitude condition for optimal cooling keeps consistency at all detunings and satisfies the condition $2\Phi_{rf} + \delta\Phi_{dc} = 8.646\,\text{m}\Phi_0 \gtrapprox \Phi_{12}$. Because the strong decoherence enlarges the transition region near Δ_{12}, the amplitude needs to be increased to longer the time in the region.

In order to compare two methods, we put them together in Fig. 10 (a). The white solid line represents the amplitude for optimal cooling in the ordinary method, while the green dashed line represents that in the new method. Actually, the green dashed line is part of the optimal region in the ordinary method with different cooling interests shown by the white dashed arrowheads. Cooling interests of the green solid line have large energy spacing and hence the influence of the thermal noise is little. However the cooling interests in the new method are bothered by the temperature due to a small spacing. Therefore the green dashed line produces great effects to realize lower effective temperature on the cooling interests.

At the detuning $\delta\Phi_{dc} = 0.05$ mΦ_0 we change the amplitude and frequency to obtain the population in state $|1\rangle$ with the new method, shown in Fig. 11 (a). Then by extracting the lowest population at each frequency in Fig. 11 (a), an unconventional phenomenon occurs that larger frequency yields better cooling as shown in Fig. 11 (b). This phenomenon disobeys the frequency condition in the ordinary method, and we would discuss this result in the next section. In addition, in Fig. 11 (b), although 5 MHz is not the frequency for optimal cooling, it also provides an effective cooling and we can still use 5 MHz for cooling in practice. Moreover at each frequency the amplitude corresponding to the lowest population in state $|1\rangle$ as shown in Fig. 11 (c), demonstrates that larger amplitude is needed to produce the optimal cooling at larger frequency. Since larger frequency results into shorter time in the transition region, larger amplitude is needed to brings more time in the transition region over one period. However more transition region covered by the microwave indicates averagely smaller transition rate described by Eq. (8). These two factors result into the behavior in Fig. 11 (c).

Furthermore, still at the detuning $\delta\Phi_{dc} = 0.05$ mΦ_0, at different dephasing rates and frequencies we vary the amplitudes to obtain the lowest population in state $|1\rangle$, as illustrated in Fig. 12. The frequency corresponding to the optimal cooling increases as the dephasing rate increases instead of staying at 5 MHz. Since the new method eliminates the disturbance of Δ_{03} which conflicts with the cooling mechanism, the condition for optimal cooling here should agree with that of the experiment. This anti-intuitive result indicates there are underlying and interesting physical mechanisms.

V. OPTIMAL MDLZ TRANSITION

To explain the strange phenomenon in Sec. IV, firstly we return to MDLZ transition and change the transition rate Eq. (9) to the form

$$W_{ij} = \frac{\Delta_{ij}^2}{2} \sum_n \frac{(2\omega/A_{ij})^{2/3}\text{Ai}^2[(2\omega/A_{ij})^{1/3}(n - A_{ij}/\omega)]}{(\varepsilon_{ij} + A_{ij} - n\omega)^2/(\Gamma_2+\gamma) + \Gamma_2 + \gamma}, \quad (10)$$

where we use the airy function Ai(x) to express the Bessel function $J_n(x) = (2/x)^{1/3} Ai[(2/x)^{1/3}(n-x)]$. The sum is determined by the terms with n, the nearest integer to $(\varepsilon_{ij} - A_{ij})/\omega$. Therefore, we have

$$\begin{aligned} W_{ij} \approx\ & \Delta_{ij}^2 (\tfrac{\omega^2}{2A^2})^{\frac{1}{3}} \text{Ai}^2[(2\omega/A)^{\frac{1}{3}}\varepsilon_{ij}/\omega]/(\Gamma_2+\gamma) + \\ & \Delta_{ij}^2 (\tfrac{1}{2A^2})^{\frac{1}{3}} \text{Ai}^2[(2\omega/A)^{\frac{1}{3}}(\varepsilon_{ij}-\omega)/\omega]/(\tfrac{\omega^{4/3}}{\Gamma_2+\gamma} + \tfrac{\Gamma_2+\gamma}{\omega^{2/3}}) + \\ & \Delta_{ij}^2 (\tfrac{1}{2A^2})^{\frac{1}{3}} \text{Ai}^2[(2\omega/A)^{\frac{1}{3}}(\varepsilon_{ij}+\omega)/\omega]/(\tfrac{\omega^{4/3}}{\Gamma_2+\gamma} + \tfrac{\Gamma_2+\gamma}{\omega^{2/3}}). \end{aligned} \quad (11)$$

Then we would use the above expression to take a qualitative analysis. Eq. (11) shows the term $\omega^{4/3}/(\Gamma_2+\gamma) + (\Gamma_2+\gamma)/\omega^{2/3}$ would increase the second and third term until the frequency reaches to nearly $(\Gamma_2+\gamma)/2\pi$ and in this process

the total transition rate would increase. This explains why under the dephasing rate $\Gamma_2/2\pi = 1$ GHz the increase of frequency from 5 MHz to 500 MHz brings the decrease of population in state $|1\rangle$ in Fig. 11 (b). As the frequency is larger than $(\Gamma_2+\gamma)/2\pi$, this term would contribute to the decrease of the transition rate W_{ij}. Therefore the frequency corresponding to the maximum of W_{ij} is relative with the decoherence rate. Since here the contribution from other term in Eq. (10) is neglected, we only give a qualitative analysis and further conclusions could not be obtained from Eq. (11).

Therefore, we return to the expression in Eq. (9). For a small dephasing rate, e. g. $\Gamma_2/2\pi = 0.05$ GHz, the frequency corresponding to the maximum of W_{ij} would be nearly 10 MHz [Fig. 13 (a)]. If the dephasing rate Γ_2 is large, e. g. $\Gamma_2/2\pi$ = 1 GHz, the maximum of W_{ij} would need a large frequency nearly 470 MHz, as shown in Fig. 13 (b). That means in this case the frequency of the maximum of W_{ij} reaches at the incoherent transition region introduced in Sec. II, not staying at nearly 5 MHz. Fig. 13 (d) is the plot of the frequency corresponding to the maximum of W_{ij} vs. the dephasing rate. The frequency increases with the dephasing rate, agreeing with the qualitative analysis. MDLZ transition rate W_{ij} depends on the driving period and the population transferred by LZ transition over one period. The two factors are both related with the microwave frequency. Larger frequency yields more times of LZ transitions in one unit time, but also brings less LZ transition population. The above qualitative and quantitive discussions demonstrate at an appropriate frequency the maximum of MDLZ transition rate can be obtained. Furthermore the decoherence has an important effect on the modulation of the appropriate frequency.

When the dephasing rate is small, e. g. $\Gamma_2/2\pi = 0.05$ GHz, at the detuning $\delta\Phi_{dc} = 0.05$ mΦ_0 the population in state $|1\rangle$ shown in Fig. 13 (c) does not at first decrease to a lowest value as W_{12} indicates in Fig. 13 (a), but exhibits a monotonic increase. This is because the population in state $|1\rangle$ near the degeneracy point is dependent on not only W_{12}, but also W_{10} and W_{23}. In this case the low frequency driving would result the low velocity near Δ_{01} and Δ_{23} such that W_{01} and W_{23} have contribution on the population in state $|1\rangle$. If we choose the detuning far away from the degeneracy point, this difference between the population in state $|1\rangle$ and W_{12} would disappear as shown in Figs. 14 (a) and 14 (b).

When the dephasing rate is large, e. g. $\Gamma_2/2\pi = 1$ GHz, the population exhibits a monotonic decrease with the frequency and does not increase again [Fig. 11 (b)]. At the detuning far away from 0 mΦ_0, the population in state $|1\rangle$ is

$$p_{11} = \frac{\Gamma_{01}^{'}}{\Gamma_{10}^{'} + \Gamma_{01}^{'} + W_{12}}, \tag{12}$$

where $\Gamma_{01}^{'} = \Gamma_{10}^{'} \exp\{-(\varepsilon_{12} - A_{12})/T\}$, and W_{ij} is defined by Eq. (9). Seen from Eq. (12), $\Gamma_{01}^{'}$ would also play an important role in the cooling. In order to produce the optimal cooling, larger frequency needs larger amplitude [Fig. 11 (c) and Fig. 15]. According to the expression of $\Gamma_{01}^{'}$ in Eq. (12), larger amplitude would result the decrease of $\Gamma_{01}^{'}$, which diminishes the population in state $|1\rangle$. Therefore, the final population exhibits different characters from W_{12}.

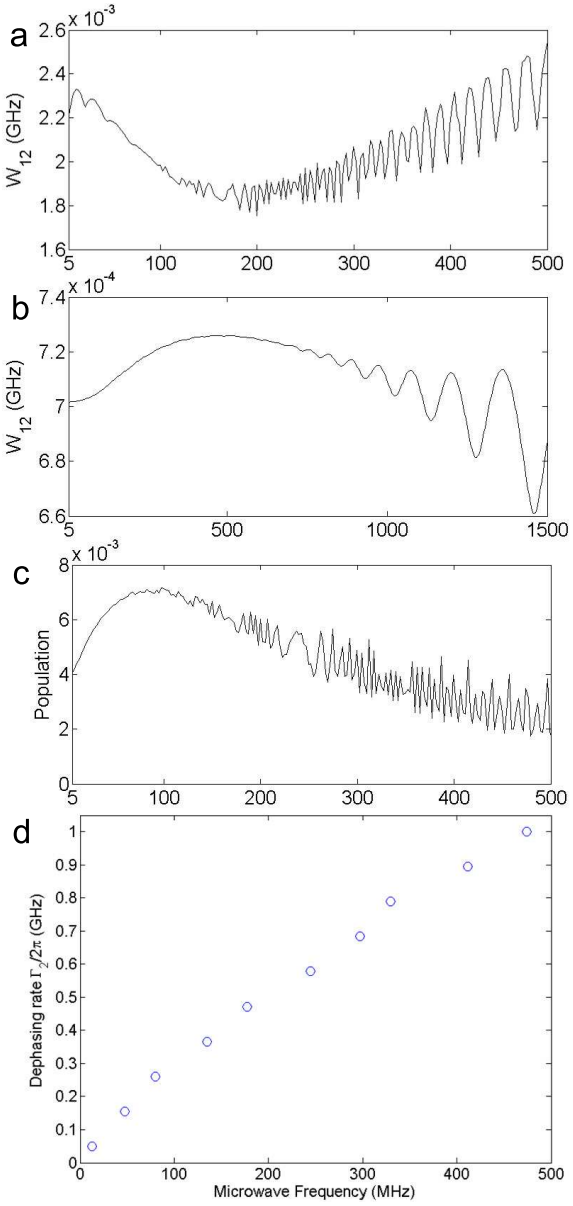

FIG. 13: (a) and (b). The maximum of W_{12} among different amplitudes at each frequency versus microwave frequency at the detuning $\delta\Phi_{dc} = 0.05$ mΦ_0 under the dephasing rate $\Gamma_2/2\pi = 0.05$ GHz and 1 GHz respectively. (c) shows the lowest population in state $|1\rangle$ among different amplitudes at each frequency and the detuning $\delta\Phi_{dc} = 0.05$ mΦ_0 under the dephasing rate $\Gamma_2/2\pi = 0.05$ GHz. (d). The frequency of the maximum of W_{12} versus the dephasing rate at the detuning $\delta\Phi_{dc} = 0.05$ mΦ_0. All figures are calculated in the new method. The other parameters are the same with those of Fig. 3.

To summarize, the decoherence modulates the frequency of the maximum of MDLZ transition rate, influencing the cooling effect. Although the incoherent transition region does not receive much attention in quantum information due to the loss of coherence, our studies show that the region has the particular advantage in quantum transition and quantum cool-

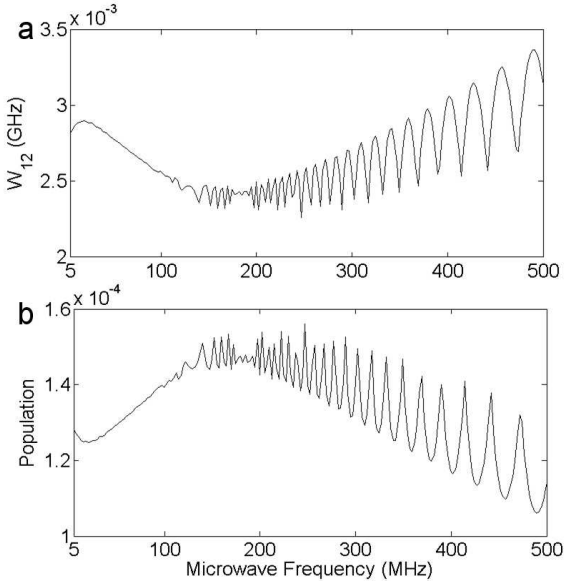

FIG. 14: (a). The maximum of W_{12} among different amplitudes at each frequency versus the frequency in the new method with the detuning $\delta\Phi_{dc} = 3\ \mathrm{m}\Phi_0$ and the dephasing rate $\Gamma_2/2\pi = 0.05$ GHz. (b). The lowest population in state $|1\rangle$ at each frequency versus the frequency with the detuning $\delta\Phi_{dc} = 3\ \mathrm{m}\Phi_0$ and the dephasing rate $\Gamma_2/2\pi = 0.05$ GHz. The other parameters are the same with those of Fig. 3.

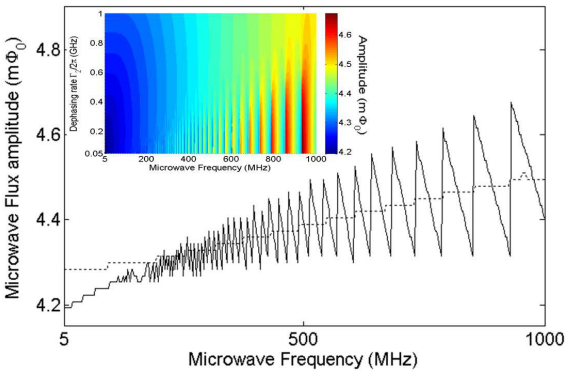

FIG. 15: (Color online) The amplitude corresponding to the maximum of W_{12} at each frequency versus the frequency in the new method with the detuning $\delta\Phi_{dc} = 0.05\ \mathrm{m}\Phi_0$ at $\Gamma_2/2\pi$ = 0.05 GHz (the solid line) and 1 GHz (the dotted line). The other parameters used here is identical with those of Fig. 3. The inset shows the amplitude corresponding to the maximum of W_{12} at each dephasing rate and frequency with the detuning $\delta\Phi_{dc} = 0.05\ \mathrm{m}\Phi_0$.

ing. This decoherence induced modulation of the maximum of MDLZ transition should also emerge in the ordinary cooling method as indicated in Eq. (11). Under the weak decoherence, e. g. $\Gamma_2/2\pi = 0.06$ GHz, at a detuning far away from Δ_{01}, e. g. $\delta\Phi_{dc} = 0.5\ \mathrm{m}\Phi_0$, even when the state is driven to completely reach the transition region near Δ_{12}, Δ_{03} would not have effects. Therefore, nonmonotonic effect of MDLZ transition can be found in the population just as shown in Fig. 6 (b) with a frequency ~ 10 MHz corresponding to the optimal cooling. However, at the detuning $\delta\Phi_{dc} = 0.05\ \mathrm{m}\Phi_0$ the amplitude of the maximum of W_{12} makes the crossover Δ_{03} effective.(see the inset of Fig. 15) Therefore, smaller amplitude is needed and results of a final frequency 5 MHz.

VI. CONCLUSION

Starting from a recent experiment, we investigate the microwave-driven cooling in an artificial atom subjected to the environment noise. Under the weak decoherence, we show that the optimal cooling at each detuning depends on not only the microwave frequency but also the amplitude. At each detuning, the frequency where the optimal cooling is achieved is not always at 5 MHz, maybe slightly larger than 5 MHz. At the same time, the optimal cooling also requires that the amplitude satisfies the relation $\Phi_{rf} \gtrapprox \Phi_{12} - \delta\Phi_{dc}$.

We further discuss the cooling under the strong decoherence, where more vibrational degrees of freedom are coupled to the two lowest states, making the ordinary cooling method ineffective. To recover the effective cooling, we present an improved cooling method, which employs a revised driving waveform to avoid another "harming" side crossover. The new method can be used to effectively improve the cooling efficiency, prepare the quantum state and suppress decoherence in multi-qubit system under not only the weak decoherence but also the strong decoherence. This robustness of effective cooling under the decoherence is useful when the qubit is employed to cool neighboring quantum systems and refrigerate the environmental degrees of freedom. In addition, small microwave frequency needed in the new method also provides the possibility to use our method on adiabatic quantum computation.

Furthermore, we show that better cooling effect is not dependent on lower frequency and the frequency for optimal cooling in both methods monotonically increases with the decoherence stronger. Currently, MDLZ transition in the coherent region has attracted lots of attentions due to coherent phenomena. We point out the incoherent transition region has the particular advantage in the cooling and MDLZ transition with both methods. Our study demonstrates qualitatively and quantitively the frequency where MDLZ transition rate reaches maximum is modulated by the decoherence and deepens the understanding to the physical mechanism of MDLZ transition as well as the optimal cooling. Moreover, the results based on MDLZ transition can be used to other systems with similar energy states structure, realizing quantum state manipulation. Especially, for systems consisting of the interaction between the qubit and the physical resonator, such as micromechanical beam, our study can further be used to achieve the optimal cooling of the qubit, or even resonators.

VII. ACKNOWLEDGEMENTS

We thank Valenzuela, S. O. for useful discussions. This work was partly supported by the State Key Program for Basic Researches of China (2011CB922104), the NSFC

(10725415), and the Natural Science Foundation of Jiangsu Province (BK2010012)..

* Electronic address: yuyang@nju.edu.cn

[1] Y. Makhlin, J. Diggins, and A. Shnirman, Rev. Mod. Phys. 73, 357 (2001).

[2] M. A. Nielsen and I. L. Chuang, *Quantum Computation and Quantum Information*, (Cambridge University Press, Cambridge, 2000).

[3] J. Q. You and F. Nori, Phys. Today 58, No. 11, 42 (2005);

[4] J. E. Mooij, Science **307**,1210 (2005)

[5] J. Clarke and F. K. Wilhelm Nature(London) **453**, 1031(2008)

[6] Y. Nakamura, Y. A. Pashkin, and J. S. Tsai, Nature(London) **398**,786(1999)

[7] D. Vion, A. Aassime, A. Cottet, P. Joyez, H. Pothier, C. Urbina, D. Esteve, and M. H. Devoret. Science **296** 886 (2002)

[8] Y. Yu, S. Y. Han, X. Chu, S. I. Chu, Z. Wang. Science **296**, 889(2002)

[9] J. M. Martinis, S. Nam, J. Aumentado, and C. Urbina. Phys. Rev. Lett. **89**,117901(2002)

[10] I. Chiorescu, Y. Nakamura, C. J. P. M. Harmans, and J. E. Mooij. Science **299**, 1869(2003)

[11] Y. Nakamura, Y. A. Pashkin, and J. S. Tsai, Phys. Rev. Lett. 87, 246601 (2001) .

[12] I. Chiorescu, P. Bertet, K. Semba, Y. Nakamura, C. J. P. M. Harmans, and J. E. Mooij, Nature (London) 431, 159 (2004)

[13] A. Wallraff, D. I. Schuster, A. Blais, L. Frunzio, R.-S. Huang, J. Majer, S. Kumar, S. M. Girvin, and R. J. Schoelkopf, Nature (London) 431, 162 (2004) .

[14] D. I. Schuster, A. A. Houck, J. A. Schreier, A. Wallraff, J. M. Gambetta, A. Blais, L. Frunzio, J. Majer, B. Johnson, M. H. Devoret, S. M. Girvin, and R. J. Schoelkopf. Nature (London) 445, 515 (2007)

[15] A. Izmalkov, M. Grajcar, E. Il'ichev, T. Wagner, H.-G. Meyer, A. Yu. Smirnov, M. H. S. Amin, A. M. van den Brink, and A. M. Zagoskin, Phys. Rev. Lett. 93, 037003 (2004)

[16] M. Grajcar, A. Izmalkov, S. H. W. van der Ploeg, S. Linzen, T. Plecenik, T. Wagner, U. Hübner, E. Il'ichev, H.-G. Meyer, A. Y. Smirnov, P. J. Love, A. M. van den Brink, M. H. S. Amin, S. Uchaikin, and A. M. Zagoskin, Phys. Rev. Lett. 96, 047006 (2006)

[17] W. D. Oliver, Y. Yu, J. C. Lee, K. K. Berggren, L. S. Levitov, and T. P. Orlando. Science **310**, 1653(2005)

[18] M. Sillanpää, T. Lehtinen, A. Paila, Y. Makhlin, and P. Hakonen. Phys. Rev. Lett. **96**,187002(2006)

[19] A. Izmalkov, S. H. W. van der Ploeg, S. N. Shevchenko, M. Grajcar, E. Il'ichev, U. Hübner, A. N. Omelyanchouk, and H. G. Meyer, Phys. Rev. Lett. 101, 017003 (2008).

[20] C. M. Wilson, T. Duty, F. Persson, M. Sandberg, G. Johansson, and P. Delsing, Phys. Rev. Lett. 98, 257003 (2007)

[21] J. Hauss, A. Fedorov, C. Hutter, A. Shnirman, and G. S. Schön, Phys. Rev. Lett. 100, 037003 (2008).

[22] M. Grajcar, S. H. W. van der Ploeg, A. Izmalkov, E. Il'ichev, H.-G. Meyer, A. Fedorov, A. Shnirman, and G. S. Schön, Nat. Phys. 4, 612 (2008).

[23] I. Martin, A. Shnirman, L. Tian, and P. Zoller, Phys. Rev. B 69, 125339 (2004)

[24] M. Grajcar, S. Ashhab, J. R. Johansson, and F. Nori, Phys. Rev. B 78, 035406 (2008)

[25] J. E. Mooij, T. P. Orlando, L. Levitov, L. Tian, C. H. van der Wal, and S. Lloyd, Science 285, 1036 (1999).

[26] I. Chiorescu, Y. Nakamura, C. J. P. M. Harmans, and J. E. Mooij, Science 299, 1869 (2003).

[27] S. O. Valenzuela, W. D. Oliver, D. M. Berns, K. K. Berggren, L. S. Levitov, T. P. Orlando, Science 314, 1589 (2006)

[28] D. J. Wineland, R. E. Drullinger, F. L. Walls, Phys. Rev.Lett. 40, 1639 (1978).

[29] W. Neuhauser, M. Hohenstatt, P. Toschek, H. Dehmelt, Phys. Rev. Lett. 41, 233 (1978).

[30] I. Marzoli, J. I. Cirac, R. Blatt, P. Zoller, Phys. Rev. A. 49, 2771 (1994).

[31] C. Monroe, D. M. Meekhof, B. E. King, S. R. Jefferts, W. M. Itano, D. J. Wineland and P. Gould, Phys. Rev. Lett. 75, 4011 (1995).

[32] S. N. Shevchenko, S. Ashhab, and F. Nori, Physics Reports **492**, 1 (2010).

[33] A. V. Shytov, D. A. Ivanov, and M. V. Feigel'man, Eur. Phys. J. B 36, 263 (2003).

[34] L. D. Landau., Phys. Z. Sowjetunion **2**, 46 (1932); G. Zener, Proc. R. Soc. London. Ser. A **137,** 696 (1932); E. C. G. Stückelberg, Helv. Phys. Acta **5,** 369 (1932).

[35] J. Ankerhold and H. Grabert, Phys. Rev. Lett. 91, 016803 (2003).

[36] G. Ithier, E. Collin, P. Joyez, D. Vion, D. Esteve, J. Ankerhold, and H. Grabert, Phys. Rev. Lett. 94, 057004 (2005).

[37] K. Saito, M. Wubs, S. Kohler, P. Hanggi, and Y. Kayanuma, Europhys. Lett. 76, 22 (2006).

[38] K. Saito and Y. Kayanuma, Phys. Rev. B 70, 201304(R) (2004).

[39] G. Z. Sun, X. D. Wen, B. Mao, J. Chen, Y. Yu, P. H. Wu, and S. Y. Han, Nat. Commun. 1:51, doi: 10.1038/ncomms1050 (2010).

[40] S. N. Shevchenko, S. H. W. van der Ploeg, M. Grajcar, E. Il'ichev, A. N. Omelyanchouk, and H.-G. Meyer, Phys. Rev. B 78, 174527 (2008).

[41] D. M. Berns, M. S. Rudner, S. O. Valenzuela, K. K. Berggren, W. D. Oliver, L. S. Levitov, and T. P. Orlando, Nature(London) **455**, 51(2008)

[42] G. Z. Sun, X. D. Wen, Y. W. Wang, S. H. Cong, J. Chen, L. Kang, W. W. Xu, Y. Yu, S. Y. Han, and P. H. Wu. Applied Physics Letters **94**,102502(2009)

[43] J. Bylander, M. S. Rudner, A. V. Shytov, S. O. Valenzuela, D. M. Berns, K. K. Berggren, L. S. Levitov, and W. D. Oliver, Phys. Rev. B 80, 220506 (2009)

[44] W. D. Oliver, S. O. Valenzuela, Quant. Info. Proc. 8, 261 (2009).

[45] D. M. Berns, W. D. Oliver, S. O. Valenzuela, A. V. Shytov, K. K. Berggren, L. S. Levitov, and T. P. Orlando, Phys. Rev. Lett. **97** ,150520(2006)

[46] L. J. Du, M. J. Wang, and Y. Yu, Phys. Rev. B 82, 045128 (2010)

[47] L. J. Du, and Y. Yu, Phys. Rev. B 82, 144524 (2010)

[48] M. S. Rudner, A.V. Shytov, L. S. Levitov, D. M. Berns, W. D. Oliver, S. O. Valenzuela, and T. P. Orlando, Phys. Rev. Lett. **101**,190502(2008)

[49] A. O. Niskanen, Y. Nakamura, and J. P. Pekola, Phys. Rev. B 76, 174523 (2007)

[50] J. Q. You, Y. X. Liu, and F. Nori, Phys. Rev. Lett. 100, 047001 (2008)

[51] M. H. S. Amin, and D. V. Averin, Phys. Rev. Lett. **100**, 197001(2008)

[52] M. H. S. Amin and F. Brito, Phys. Rev. B 80, 214302 (2009)

[53] L. J. Du, and Y. Yu, in preparation.